PROCESSING AND TESTING OF THERMOPLASTIC COMPOSITE CYLINDRICAL SHELLS FABRICATED BY AUTOMATED FIBER PLACEMENT

A. Bruce Hulcher
NASA Marshall Space Flight Center, Huntsville, AL 35812

David M. McGowan and Brian W. Grimsley
NASA Langley Research Center, Hampton, VA 23681

Norman J. Johnston
Old Dominion University, Norfolk, VA 23529

ABSTRACT

Two 61-cm-diameter eight-ply quasi-isotropic IM7/PEEK cylindrical shells were fabricated by automated fiber placement the NASA Langley Research Center using only infrared radiant heat to preheat the substrate and incoming composite uni-tape. The shells were characterized by ultrasonic c-scans for overall consolidation quality, and by optical microscopy and acid digestion for void content. Compression tests were also performed. Although the material used in the study was of generally poor quality due to numerous splits and dry fiber regions, the process was able to achieve a net reduction in void content in the as-placed component. Microscopy of the composite shells revealed well-consolidated, void-free interfaces. The two cylinders were then tested in uni-axial compression in a 1334 kN-capacity hydraulic test machine until buckling occurred. A geometrically nonlinear finite element analysis was conducted, and the differences between the predicted and measured values were 18.0 and 25.8 percent, respectively. Inclusion of measured imperfections of the cylinder into the analysis is expected to reduce these differences.

KEY WORDS: Thermoplastics, Fiber Placement

1.0 INTRODUCTION

The successful in-situ fabrication of large, high quality composite structures is critical for the development of the next generation of reusable launch vehicles. Structures such as cryogenic fuel tanks, with dimensions of 9 m in diameter and 18 m in length, must be fabricated. Autoclave fabrication of composite structures includes expenses associated with hand lay-up, tooling and autoclave time. These costs increase rapidly with part size and complexity. Fabrication of composite articles from materials with high-temperature matrix resin systems introduces further problems associated with the large thermal expansion of the tooling materials. The ability to successfully fabricate net-shape, fully-consolidated composite structures with such methods as automated fiber placement will enable significant savings in overall costs. Autoclave processing of such structures would be prohibitively expensive due to the need for appropriately sized autoclaves and support tooling. Autoclaves of the size needed to cure the largest proposed tanks do not now exist. Prior to the fabrication of full-scale structures for these applications, in-situ processing of these materials must be perfected on a small scale. As part of this effort, NASA Langley Research Center is conducting research into fiber-placement of closed-section, carbon fiber-reinforced thermoplastic cylindrical shells.

The fabrication of 61-cm-diameter, eight-ply quasi-isotropic shells by fiber-placement was conducted in the present study. Previous fabrication efforts at the Langley placement facility have utilized hot gas and hot gas/infrared (IR) radiation to heat the incoming composite tape and substrate prior to compaction and consolidation by a heated compaction roller [1,2]. IR radiant heating was investigated as a means of raising the nip point temperature; stagnation of the gas flow at the nip region was shown to limit the effectiveness of heated gas for material preheating. The ability to fabricate well-consolidated composites by fiber placement with IR energy as the sole pre-heating source had not been investigated. Initial placement trials indicated that good interfacial bonding and consolidation could be attained with IR heating alone.

Although the process was unable to fully heal the splits and dry fiber regions within the supplied uni-tape, a net reduction in void content was obtained in subsequent testing. The cylindrical shells were subsequently tested in uni-axial compression to failure. The results indicate that the fiber-placed shells failed at relatively high percentages of predicted analytical values of the failure load as predicted for perfect (i.e., flawless) shells.

2.0 EXPERIMENTAL

2.1 General

2.1.1 Material [2] The material used for cylindrical shell fabrication was supplied by Cytec Fiberite and consisted of the semi-crystalline polymer matrix PEEK (T_g = 145°C, T_m = 342°C) and IM7 fibers [3]. This material was supplied in preimpregnated tape form with nominal thickness and width dimensions of .015 and 3.17 cm, respectively. According to material certifications, this tape had an average resin content of 32% by weight and an average fiber areal weight of 145 g/m^2.

[2] The use of trademarks or names of manufacturers in this report is for accurate reporting and does not constitute an official endorsement, either expressed or implied, of such products or manufacturers by NASA.

A photomicrograph of the as-received PEEK/IM7 tape is shown in Figure 1. This tape was found to have high void content, uneven fiber distribution resulting in resin-rich areas, and an irregular tape surface. Other flaws including tape splits and dry spots which were not clearly evident in the figure were observed in other material samples.

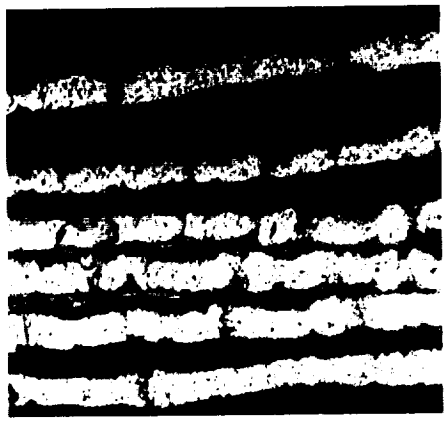

Figure 1. Optical micrograph of as-received PEEK/IM-7 tape. Six samples are shown. Tape thickness is 0.016 cm.

2.1.2 Fiber Placement Facility The placement facility at the NASA Langley Research Center consists of a six-axis industrial robot which has been fitted with a heated placement head. Composite material in tape form is fed to the compaction roller where it is heated and forced into intimate contact with the substrate ply. Fabrication capabilities include both flat panel and cylindrical geometries. Tooling is available such that cylindrical shells may be fabricated having inside diameters of 14.6 cm, 45.7 cm, and 61 cm. Fabrication of cylindrical shells requires the use of contoured compaction rollers for plies other than 90° [4].

2.2 Process Development and Fabrication – Cylindrical Shell # 1

2.2.1 Peel Tests The wedge peel test method was developed at the NASA Langley Research Center for rapid quantitative determination of the interfacial consolidation quality for fiber placed thermoplastic materials[5]. Peel specimens were fabricated to determine the optimal placement parameters in the process development for the current study. These specimens were placed on the same tool used to fabricate the cylinder in an attempt to simulate the thermal boundary condition of the tool surface as during actual shell placement. Two-ply unidirectional peel specimens 45.7 cm long were placed in the cylinder hoop (90°) direction. Placement speed, and compaction roller temperature were varied. The IR lamp output was held constant at 100% throughout the study, and the compaction load was also held constant at 445 N.

It was clear from the results of the peel testing that placement at a rate of 5.10 cm/sec with a 300°C compaction roller is roughly equivalent to placement at 6.35 cm/sec with a 330°C roller. Since higher throughputs are advantageous, the placement parameters chosen for cylinder fabrication are those at the higher speeds. It should be noted that at wedge peel loads generally

above 5.25 kN/m, cohesive failure of the specimen occurs. With cohesive failure, the peel plane wanders from the ply interface and initiates failure within the composite ply. Four of the five specimens placed at the higher roller temperature value failed cohesively, indicating near-optimal processing of the ply interfaces.

2.2.2 Off-Axis Ply-Ply Bond Tests In wedge peel specimens having plies with fiber direction other than parallel to the peel direction, the matrix is not able to handle the stress. This effect leads to a premature failure of the specimen during testing. An alternative approach that was considered for the off-axis specimens was flatwise tensile testing. In this test, the specimen ply direction is not a factor, since loading is normal to the tape surface. A [90°/0°] specimen was prepared by bonding a 1.27 x 1.91 cm sample to the faces of two loading blocks. The specimen was fabricated with a compaction load of 445 N, a placement processing rate of 6.35 cm/sec., and a compaction roller temperature of 330°C. Hysol 934 epoxy adhesive was used to bond the loading blocks to the specimen. Surface preparation included grit blasting and cleaning with methyl-ethyl-ketone (MEK) prior to bonding. A crosshead speed of .0254 cm/min. was used during testing. A peak load of 3.1 kN, equivalent to a stress of 12.89 MPa, was attained. Inspection of the composite plies revealed approximately 25% of the specimen area failed at the ply interface. The primary failure was due to de-bonding at the adhesive-composite interface. Due to the strength of the composite in resisting the flatwise tensile load and the adhesive failure at the loading block/composite interface, it was decided that void content analysis alone be used for further process development.

2.2.3 Specimen Microscopy Specimens of each of the 3 ply interfaces (90°/90°), (90°/0°) and (45°/0°) were potted and polished for microscopic inspection. Visual observation of the specimens revealed very well-consolidated interfaces for all three samples. For the (90°/90°) specimen, the processing conditions which gave the lowest void content in both the tape and ply interface were 5.10 cm/sec placement speed, and 300°C compaction roller temperature. Increasing the compaction load to 667 N for each of the cross-ply specimens brought about a marked decrease in interfacial voids. Additionally, this increase in load tended to minimize upper ply surface roughness, making intimate contact and healing of the interfaces easier to achieve.

Photomicrographs were assessed qualitatively for each of the specimen interfaces in terms of interfacial void content. The compaction load, placement rate and roller temperature for each interface that resulted in the highest consolidation quality at the ply interfaces are presented in Table 1.

Table 1. Optimal processing parameters as determined by optical microscopy. IR lamp output constant at 100%.

Ply Interface	Compaction Load (N)	Placement Speed (cm/sec)	Roller Temperature (°C)
90°/90°	445	5.10	300
90°/0°	668	6.35	330
45°/0°	668	6.35	330

2.2.4 Cylinder Fabrication As mentioned in the introduction, the cylindrical shell was an eight-ply, quasi-isotropic lay-up, 61 cm in diameter, with an as-placed length of 91cm. The nominal lamination stacking sequence was $[+45°/-45°/0°/90°]_s$ The software controlling the fiber placement was set to adjust ply fiber angles based on tape width and cylinder circumference such that gaps or overlaps were minimized. Placement of the 90° plies are accomplished by 'winding' the tape down the length of the cylinder, resulting in a small deviation from 90° in the ply angle. In an attempt to balance the layup, the first hoop ply was placed at +90° and the second at -90°. The placement control files were programmed to account for the change in cylinder diameter with each additional ply, resulting in slightly different angles for the hoop plies and for the first and last two $\pm$ 45° plies. The nominal ply angles and the actual ply angles used in the shell fabrication are listed in Table 2.

Table 2. Nominal and actual ply angles for 61 cm diameter cylindrical shell placement with 3.18 cm wide tape.

Nominal Ply Angle	Actual Ply Angle
+45°	+44.8004°
-45°	-44.8004°
0°	0°
90°	+89.0515°
90°	-89.0501°
0°	0°
-45°	-44.9727°
+45°	+45.0013°

During placement of the 90° hoop plies, the roller and cylindrical placement tool axes are parallel and hence the roller is in line contact with the tool surface. Placement at angles other than 90° requires the use of contoured compaction rollers to match cylinder curvature. Separate contoured rollers are necessary for each of the 0° and $\pm$ 45° plies.

Since the cylindrical tool surface is coated with teflon, it was not possible to affect ply bonding to the tool surface. In order to create an area onto which the first ply might adhere, a layer of kapton film was applied at each end of the tool. Emery paper was used to roughen the film surface to promote ply sticking. In a first attempt, the film was taped only on the outside edge of the cylinder. This may have enabled both axial and circumferential displacement of the film during placement due to the unrestrained film edge, creating gaps in the ply. This film was discarded and replaced by Kapton tape. The cylinder placement control files were modified to increase the placement length, enabling a greater Kapton-to-composite contact length. The roller temperature was increased from 330°C to 360°C in an effort to offset the heat sink created by the aluminum tooling. This allowed for greater resin flow and enabled the strips to conform more closely to the tool surface. Prior to removal of the tool from the composite shell, it was necessary to de-bond both ends of the inner shell surface from the Kapton tape and the tool. This was accomplished by sliding a spatula between the tool and the composite shell at each end of the

composite. The tool and composite were then placed into a freezer overnight; thermal shrinkage of the tool enabled the removal of the composite shell.

*2.2.5 **Results and Discussion*** To prepare the cylinder for ultrasonic evaluation, it was necessary to machine one end to sit flat against the floor of the scanning machine. The cylinder was trimmed just beyond where the Kapton tape was located during placement. The machine used to scan the shell was a Testech Bridge, model #LS-98 ultrasonic scanner. An unattenuated beam power of E=4 was necessary to achieve adequate transmission through the wall of the composite shell. For most autoclaved composite panels, an attenuated power of E=1 is adequate for transmittal of the signal through the material. This would indicate that the shell was poorly consolidated and of high void content. The scan of this shell is presented in Figure 2.

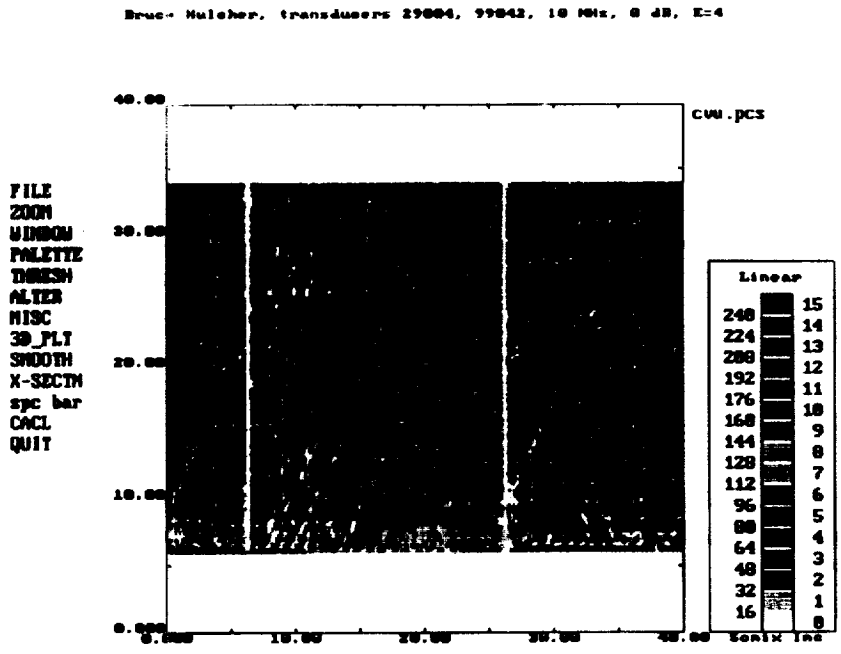

Figure 2. Ultrasonic C-scan of first composite shell. Vertical lines are artifacts of the support hardware. Scan power, E=4. The cylinder longitudinal axis is vertical in the figure.

Specimens machined from the cutoff end of the cylinder were potted and polished for analysis by optical microscopy. Two specimens each from opposing sides of the cylinder were prepared. A typical cross-section is shown in Figure 3 below. It is clear from the ultrasonic scan of the cylinder that overall consolidation was poor and the photomicrographs tend to support this conclusion. The as-received composite tape was observed visually and found to have numerous dry fiber areas and splits. Due to the very short processing times associated with fiber placement, dry fiber areas are difficult to fully wet-out and consolidate. Further process development aimed

toward increasing consolidation quality, primarily by healing tape splits was performed in preparation for the fabrication of the second composite shell.

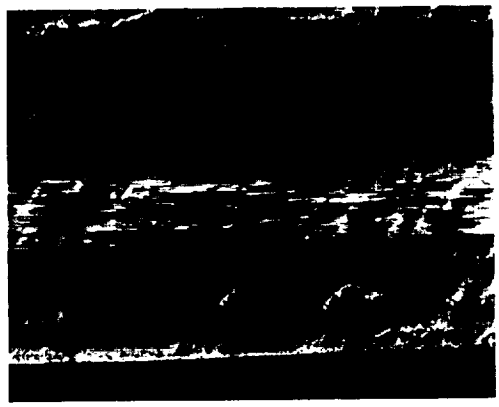

Figure 3. Photomicrograph of the as-placed 8-ply cylinder wall cross-section of composite shell #1.

2.3 Process Development and Fabrication – Cylindrical Shell #2

2.3.1 Tape Split Reduction and Peel Testing In an effort to reduce tape splits, several single strips were placed onto a flat tool surface at increased roller temperatures and compaction loads. After strip placement the specimens were visually inspected to determine split reduction. The processing conditions at which maximum split reduction was observed were as follows:

Roller Temperature	400°C
Compaction Load	1.34 kN
Placement Rate	3.05 cm/sec
IR Lamp Output Power	100%

Four wedge peel specimens were fabricated and tested at these processing conditions. The average peak failure load was 11.4 kN/m and the average propagation load was 5.4 kN/m. These values were comparable to the highest values obtained for the first cylinder process development. Cohesive failure was observed in all of these specimens, indicating maximum interfacial strength.

2.3.2 Short Beam Shear (SBS) and Flexural Property Data Unidirectional panels were fabricated using the above processing conditions defined in the previous section for mechanical property testing. The data are presented in Table 3.

Table 3. SBS and 0° flexural properties of unidirectional panels fabricated with 400°C roller and 1.34 kN compaction load.

	Short Beam Shear Strength (GPa)	0° Flexural Modulus (GPa)	0° Flexural Strength (GPa)
Literature*	0.11	148	2.04
Fiber Placement	0.054	143	1.23
Percent of Literature	50%	97%	60%

* - These values are for autoclave-cured and press-molded composites [6,7].

With the exception of the flexural modulus, which was 97% of the values for autoclave-cured composites, the data are quite low. The short beam shear test is known to be an inadequate test for interlaminar shear properties. This is due to the high compressive stress concentrations in the vicinity of the loading rollers which leads to crushing failures, and to the complex failure modes that have been witnessed for this test [8]. Again, the presence of large dry fiber regions and voids in the precursor tape material is thought to be the reason behind these low values.

2.3.3 Cylinder Fabrication Due to the higher compaction loads and roller temperatures, adhesion of the composite tape to the compaction roller increased. Contoured trailing shoes were machined and used to follow the compaction roller during fiber placement. The use of these shoes reduced ply wrinkling and provided a much smoother surface to the composite during fabrication. Additionally, roller fouling due to matrix and fiber adhesion was greatly minimized.

As with the first cylinder, the placement of the first ply was again complicated by the lack of bonding to the tool surface. At higher roller temperatures and pressures, an increase in flow resulted in wrinkling and displacement of previously placed strips, leading to unacceptable gaps between strips. For placement of plies 2-8, the parameters of section 2.3.1, which gave maximum split reduction, were employed. An increase in roller temperature and compaction force caused an increase in the tape width due to improved resin flow. The placement processing control files were altered to account for this increased width.

2.3.4 Results and Discussion The second cylinder was prepared for ultrasonic c-scan analysis as per the previous cylinder. The scan is presented in Figure 4. This scan was made at a scan energy of E=2. The results of the scan indicate a marked improvement in consolidation over the first cylinder, which was scanned at an energy of E = 4.

3.0 RESULTS AND DISCUSSION

3.1 Compression Test Results

Compression tests were performed on specimens machined from both cylindrical shells [9]. Five specimens were cut from both ends of each shell resulting in 10 specimens per shell. The as-tested specimen were 1.27 cm wide and 8.0 cm long and were tested without tabs. The crosshead speed was set at 0.127 cm/min. The specimens were observed to fail by delamination brooming. Though performing this test on tabbed specimens would likely have eliminated the brooming failures, the data was considered useful for comparison purposes. This data is presented below in Figure 5. The average values for compression strength for the first and

second cylinders were 161.2 and 229.5 MPa, respectively, indicating that the second shell had the much higher consolidation quality

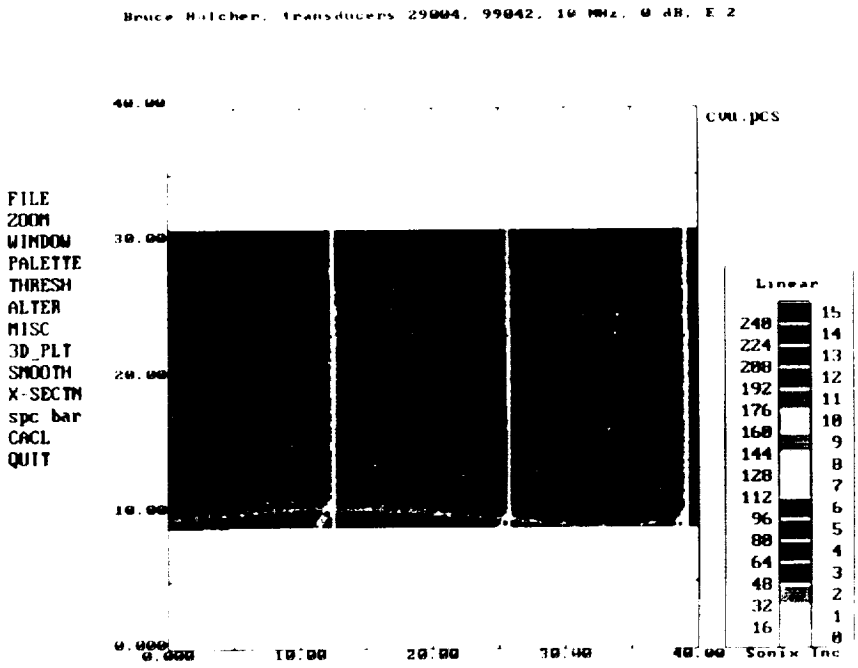

Figure 4. Ultrasonic C-scan of second composite shell. Vertical lines are artifacts of the shell support hardware. Scan power, E = 2.

3.2 Void Content Analysis

Presented in Figure 5 are the void contents of the as-received PEEK/IM7 tape, the 0° flex and SBS panels for the process development of the second shell, and each of the fiber-placed shells. The void content analysis was performed by acid digestion in accordance with ASTM standards [10] .

3.3 Discussion

3.3.1 Cylinder Fabrication The compression tests results indicate that the second composite shell was of higher consolidation quality than the first. Although the failure mechanism was brooming at the specimen end, both sets of specimens failed in like manner. As mentioned previously, had specimens been tabbed appropriately, this failure mode would likely have been avoided. The data is useful, however, for comparison purposes between the two shells. The data for the second shell represent a 30% increase in strength over the first shell, indicating a greater degree of consolidation in this matrix-dominated test The low standard deviations (less than 10%) of both data also suggest that the shells are relatively uniform with respect to consolidation quality.

Probably the most useful data in terms of both shell quality assessment and providing insight into the overall shell fabrication process is that provided by the void content data presented in Figure 5. In addition to the through-thickness splits that were evident upon visual inspection of the as-received material, micrographic examination revealed numerous areas of dry fibers. The

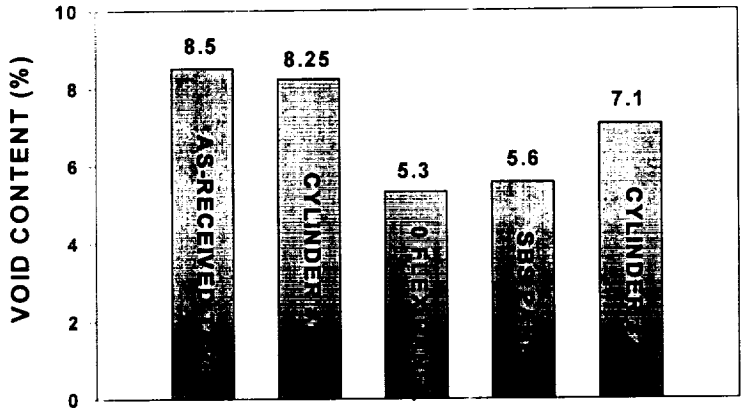

Figure 5. Void volume as determined by acid digestion.

as-received composite tape was found to have a void content of 8.5%. The void content of the first shell was essentially unchanged compared to the precursor material. The high wedge peel values along with the observed cohesive failure of those specimens with higher peel strengths led to the conclusion that the ply interfaces were well consolidated and void-free. Photomicrographs of the first shell reinforce this conclusion. This indicates that the infrared radiant heat source alone is adequate for PEEK material preheating and subsequent interfacial consolidation and that the great majority of voids in the first shell were present in the as-received material.

The SBS and 0°flex panels which were fabricated at higher roller temperatures and compaction loads, had the lowest void content of any of the specimens tested. These data represent an average reduction of 35% in void volume over the as-received material. The second shell however, which was fabricated at the same conditions as the SBS and flex panels, had a void volume of 7.1%. Several factors may help to explain the discrepancy. The unidirectional layup of the SBS and flex panels allow fibers to nest at the interfaces, increasing interfacial bond quality by lowering the void content at the interfaces. The higher void content of the shell could be due to the increase in scattering of the infrared radiation due to substrate curvature. This would reduce the amount of radiant energy available for material pre-heating. Another possible source of discrepancy are the contoured compaction rollers used for placement of the $\pm$ 45° and 0° plies. Each of these rollers is machined for use on a 61-cm-diameter surface. Placement of each additional ply increases the actual working diameter of the surface. This effect would result in areas of high and low pressure across the contact length of the roller due to the curvature

mismatch. Such a pressure gradient would reduce the ability of the roller to fully consolidate the laminate.

Photomicrographs shown in Figure 6 reveal the presence of large regions of dry fibers within the composite tape. Since material heating, intimate contact, interfacial healing and consolidation during fabrication must occur within a span of tens of milliseconds in the fiber placement process, flow and wet-out of these dry areas is highly improbable. For this reason, maximum void content, along with other specifications, have been proposed for ribbon and tape used in thermoplastic fiber placement processing of advanced composites [11].

A micrograph of the second shell is shown in Figure 7, followed by a photograph of the completed shell in Figure 8.

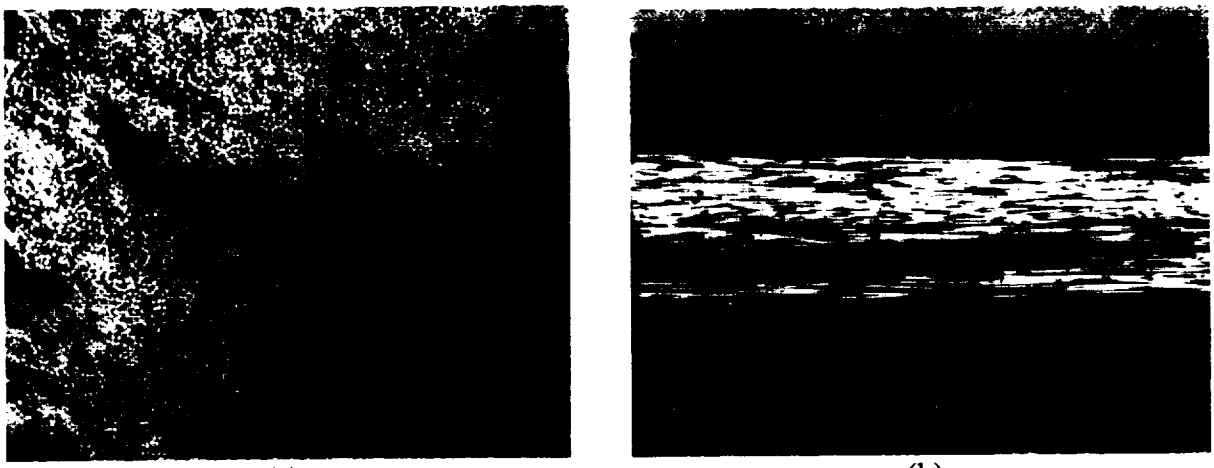

Figure 6. Micrographs of 0° flex specimen showing typical dry fiber areas. Large dry fiber area in (b) is located in lower 90° ply at center of figure.

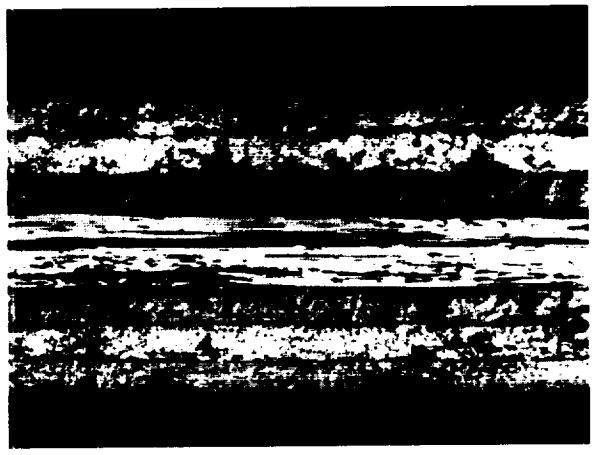

Figure 7. Micrograph of typical section of second cylinder.

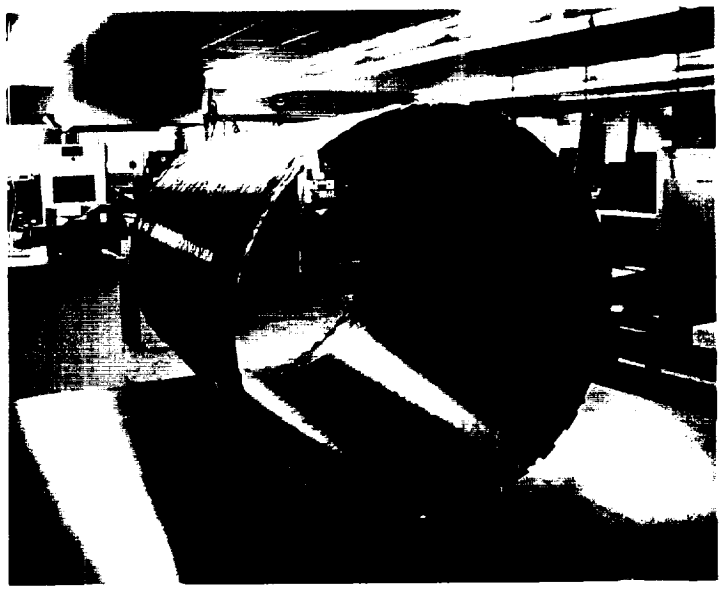

Figure 10. Second composite shell after removal of placement tool.

3.3.2 Cylinder Uni-Axial Compression Testing

3.3.2.1 Apparatus and Testing The two cylinders were each tested in uni-axial compression in a 1334-kN-capacity hydraulic test machine until buckling occurred. In both tests, the loaded ends of the cylinder were potted in 2.54 cm deep epoxy resin material to prevent an end brooming failure. The potted loaded ends were machined flat and parallel to each other to assure that a uniform load was applied to the cylinders. A photograph of one of the cylinders prepared for testing is shown in Figure 11. Prior to testing, the external and internal surfaces of the cylinders were digitally-mapped to determine the initial geometric imperfections and thickness variations in the cylinders. Strains were measured using 64 electrical resistance strain gages. Direct-current displacement transducers (DCDT's) were used to measure out-of-plane displacements of the cylinder wall at selected locations, as well as the displacement of the test machine loading platen. The axial load applied to the panel was measured using the test machine load cell. The strain-gage, DCDT, and load data were recorded using a high-data-rate data acquisition system. Data were taken at one-second intervals during loading only. Shadow moiré interferometry was used to monitor out-of-plane wall displacements over a portion of the external surface of the cylinders. The moiré fringe patterns were recorded using both still and video photography.

3.3.2.2 Analytical Model A geometrically nonlinear finite element analysis was conducted using the Structural Analysis of General Shells (STAGS) code [12]. This finite element model has 6,232 nodes, 6,080 quadrilateral shell elements, and 37,392 active degrees of freedom. This model was developed to be consistent with the experimental test conditions. The full length of the cylinder (including potting) was modeled. The analytical results described herein are for a geometrically perfect cylinder; no measured imperfections were included in the analytical model.

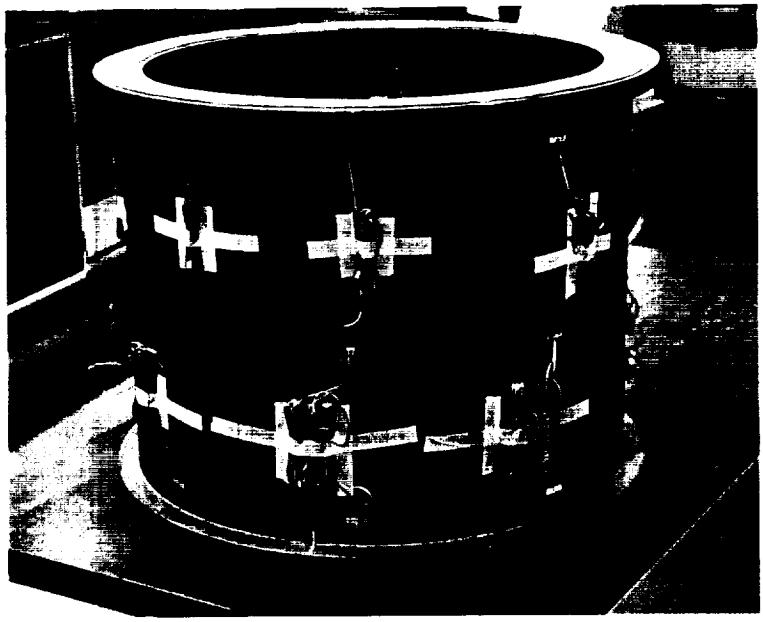

Figure 11. Eight-ply quasi-isotropic PEEK/IM7 thermoplastic composite cylindrical shell prior to uni-axial compression testing at the NASA Langley Structures and Materials Laboratory.

The boundary conditions applied to the analytical model reflect the experimental loading condition and the displacement constraints provided by the end potting. The bottom edge of the model was fully constrained. The top edge of the model had a uniform displacement in the axial direction with all other degrees-of-freedom constrained. To simulate the restraint of the potting material, the displacement in the direction normal to the wall was constrained to be zero at the nodes located within one inch from the top and bottom edges of the shell finite element model.

The analysis model was loaded with a concentrated force applied at a node on the top edge of the model. This force was distributed over the cross-section of the model by the constraint that specified that the entire top edge have a uniform end-shortening displacement. Nonlinear analyses were performed using the load computational procedure within STAGS.

3.3.2.3 Experimental Results Experimental and analytical results are presented for the tests of both cylinders. The predicted buckling load of the cylinders using the geometrically nonlinear analysis described previously was 224 kN. The experimentally determined buckling loads for shells 1 and 2 were 166 kN and 184 kN, respectively. The differences between the predicted and measured values are 25.8% and 18.0%, respectively. These differences are attributed to two factors. First, as mentioned previously, the analytical results do not account for any measured imperfections in the cylinder. Hilburger, et al. showed that highly accurate predictions of the cylinder response could be obtained by inclusion of various measured imperfections [13]. Furthermore, they showed that the inclusion of the cylinder imperfections in the analysis can reduce the predicted buckling load for a compression-loaded cylinder by as much as 30 percent.

Second, a post-test inspection of the test machine revealed that a slight eccentricity in the loading of the cylinders was present during the tests. These two factors may account for a large portion of the differences between the predicted and measured values of the cylinder buckling loads.

4.0 CONCLUSIONS

Two cylindrical shells were fabricated from PEEK/IM7 by automated fiber placement at the NASA Langley Research Center fiber placement facility. The goals of the study were to in-situ fabricate well-consolidated thermoplastic shells using infrared radiation as the sole material pre-heating source and to gain experience in the fiber placement of thermoplastic cylindrical shells.

The limiting factor in the fiber placement of high quality, well-consolidated shells in the present study was the poor quality of the composite tape supplied to the placement machine. The inability to move resin into the numerous dry regions of the tape resulted in a minimal decrease in the high void content of the precursor material. Micrographic inspection of both shell laminates revealed good consolidation quality at the ply interfaces, however. Since the degree of interfacial consolidation is largely a function of the adequacy of the preheating of the incoming and substrate materials, the use of IR heat alone was shown to be effective. The use of a contoured trailing shoe to prevent material from being pulled away from the substrate by roller sticking was also thought to be important to laminate quality. The shoe was observed to prevent ply wrinkling, providing a smooth surface for lamination of subsequent plies.

The two composite cylinders described herein were fabricated, tested, and analyzed at NASA Langley Research Center. Analytical predictions of the buckling loads of these two cylinders were obtained from a geometrically nonlinear analysis of a perfect cylinder. These results differ from the experimental results by 25.8% and 18.0% for composite shells 1 and 2, respectively. Inclusion of measured imperfections of the cylinder into the analysis is expected to reduce these differences.

5.0 REFERENCES

1. Grenoble, R.W., Tiwari, S.N., Marchello, J.M., Johnston, N.J., "Hybrid IR-Gas Heater for Automated Tow Placement ", 43rd International SAMPE Symposium, pp.1966-1978, May31-June 4, 1998.
2. Grenoble, R.W., "IR-Hot Gas Heat Source for Automated Tow Placement, Master's Thesis, Old Dominion University, 1998.
3. Engineered Materials Handbook - Composites, publ. ASM International, 1987.
4. Towell, T.W., Johnston N.J., Grenoble, R.W., Marchello, J.M., "Thermoplastic Fiber Placement Machine for Materials and Processing Evaluations", 41st International SAMPE Symposium, March, 1996.
5. Hulcher, A.B., Marchello, J.M., Hinkley, J.A., "Wedge Peel Testing for Automated Fiber Placement," Journal of Advanced Materials, 31 (3), July 1999, pp. 37-43.

6. High Performance Thermoplastic Resins and Their Composites, Beland, S., publ. Noyes Data Corp., 1991.
7. Thermoplastic Composite Materials - Composite Materials Series, 7, Carlsson, L.E., publ. Elsevier, 1991.
8. Whitney, J.M., Browning, C.E., "On Short Beam Shear Tests for Composite Materials," 5th International Congress on Experimental Mechanics, Montreal, Quebec, June 10-15, 1984.
9. ASTM D 695-96, " Standard Test Method for Compressive Properties of Rigid Plastics."
10. ASTM D3171-76, " Standard Test Method for Fiber Content of Resin-Matrix Composites by Matrix Digestion".
11. Hulcher, A.B., Marchello, J.M., Hinkley, J.A., Johnston, N.J., "Dry Ribbon for Heated Head Automated Fiber Placement, ", 44th International SAMPE Symposium, pp. 146-155, May 23-27, 1999.
12. Rankin, C. C., Brogan, F. A., Loden, W. A., and Cabiness, H. D., "STAGS User Manual, Version 3.0," Lockheed Martin Missiles & Space Co., Inc., Rept. LMSC P032594, March 1999.
13. Hilburger, M. W., and Starnes, J. H. Jr., "High-Fidelity Analysis of Compression-Loaded Composite Shell," Proceedings of the 42nd AIAA/ASME/ASCE/AHS/ASC Structures, Structural Dynamics and Materials Conference, Seattle, WA, April 2001. AIAA Paper No. 2001-1394.

ACKNOWLEDGEMENTS

The authors thank the following persons for their help and assistance with this study: John Kirtley and Pert Razon of NASA Langley and Will Banks of Old Dominion University for help in cylinder placement and Meg Holloman of MPDS/NASA Langley Research Center, for cylinder ultrasonic scanning testing.